

Lasers in Manufacturing Conference 2015

Glass Processing with High Power Q-Switch CO₂ Laser Radiation

Sebastian Heidrich^{a*}, Christian Weingarten^a; Emrah Uluz^b, Reinhart Poprawe^c

^a Fraunhofer Institute for Laser Technology ILT, Steinbachstr. 15, 52074 Aachen, Germany

^bNTA Isny, Seidenstraße 12-35, 88316 Isny i.A., Germany

^cChair for Laser Technology, RWTH Aachen University, Steinbachstr. 15, 52074 Aachen, Germany

Abstract

Recent results of glass processing with a prototype high power Q-switch CO₂ laser source with a maximum output power of $P_{Lmax,cw} \approx 190$ W are presented. For this, several glass materials (fused silica, BK7, S-TIH6, S-FPL53) are investigated and results regarding the achieved ablation rate and the resulting roughness are compared amongst each other. Moreover, an analysis of the chemical composition of the ablated surface is conducted and the relevance of these results for several industrial applications is discussed.

Micro Processing; Ablation; Processing of Transparent Materials

1. Motivation

Processing glass with laser radiation, compared to conventional processing, offers several advantages, e.g. locally selective processing with high flexibility and high lateral and vertical resolution. Glass ablation by laser radiation can be realized either by nonlinear effects when using ultra-short pulse lasers or by heating and evaporating the material when using CO₂ lasers. Especially Q-Switch CO₂ lasers are used for ablation and marking processes, but they are limited to small ablation rates due to their relatively low average power of $P_L \leq 50$ W [Xie et. al., 2011]. A newly developed high power Q-Switch CO₂ laser with an average output power $P_L \leq 190$ W [Staupendahl, 2014] offers a flexible approach for processing glass materials, especially with larger ablation rates and thus shorter processing times. Moreover, due to the pulse time $t_{pulse} \geq 350$ ns, in comparison to cw CO₂ laser radiation, glass materials with several chemical elements and also high thermal expansion coefficient can be processed as well [Lee, 2002]. Possible applications for this laser source are

* Corresponding author. Tel.: +49 241 8906 645; fax: +49 241 8906 121.
E-mail address: Sebastian.heidrich@ilt.fraunhofer.der

surface marking, e.g. for design purposes, and ablating, e.g. for flexibly generating of complex forms or for lightweight design.

2. Experimental setup

The experimental setup is shown in Fig. 1. The laser radiation is guided through a 2D galvanometer based scanner system which is mounted above the glass sample to be processed. The glass sample can be positioned in three dimensions using x-y-z-axes. The laser beam is focused using an F-Theta lens with a focal length of $f = 200$ mm. An extraction system in combination with a crossjet is used to remove the ablated glass material from the processing area in order to prevent environmental contamination and to ensure a stable process.

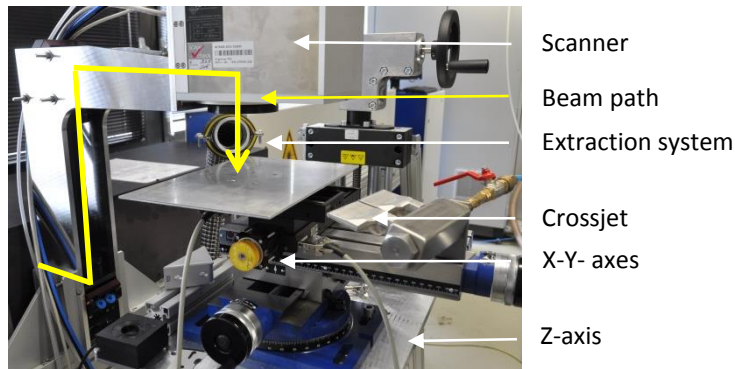


Fig. 1: Photograph of the experimental setup

For carrying out the experiments, a prototype high power Q-switch CO₂ laser source with a current maximum output power of $P_{Lmax,cw} \approx 190$ W built by FEHA LaserTec GmbH is used. Its design is described in [Staupendahl 2014], an overview of current relevant specifications of the laser source used for the experiments is given in Table 1.

Table 1 Specifications of the prototype high power Q-Switch CO₂ laser source [Feha, 2015]

Output beam diameter d [mm]	Beam quality M^2	Max. output power $P_{Lmax,cw}$ [W]	Max. peak pulse power $P_{Lmax,peak}$ [KW]	Max. repetition rate $f_{rep,max}$ [KHz]
13	< 1.33	≈ 190	40	150

Main advantage of this laser source compared to other CO₂ laser sources is its short pulse duration of $t_{pulse} \geq 350$ ns in combination with its high output power and the resulting high peak power of up to $P_{Lmax,peak} \approx 40$ KW which can be used for high ablation rates even when processing glass materials with high thermal expansion coefficient. As mentioned, a prototype is used, so the values of the final laser source, e.g. the maximum output power, will be subject to change.

3. Process parameters

The main process parameters for ablating glass material with pulsed CO₂ laser radiation are schematically shown in Fig. 2. During this process, CO₂ laser radiation is used to heat up the glass material to evaporation temperature and, therefore, locally ablate it from the glass surface. A detailed description of the process parameters and its influence on the ablation result is given in [Heidrich, 2014].

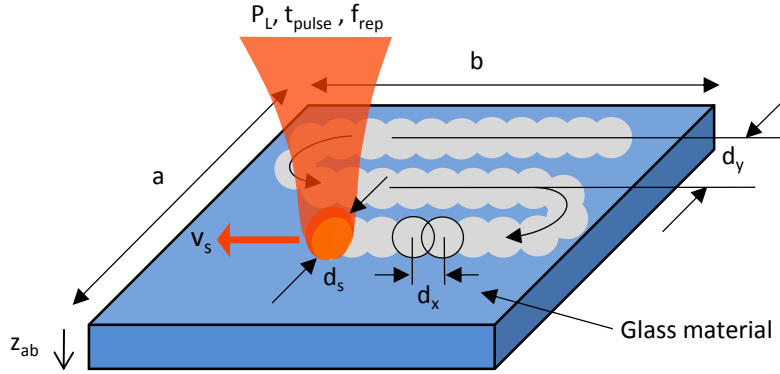


Fig. 2: Schematic drawing of the main process parameters [Heidrich 2014]

In Fig. 2, the focused laser radiation with the laser power P_L , pulse time t_{pulse} , repetition rate f_{rep} and focus diameter d_s is moved across the glass surface at the scan speed v_s in a meander scan strategy. For a coherent ablated surface, the track pitch d_y and also the pulse distance d_x , calculated with Eq. 1, are set to values smaller than d_s , so that contiguous areas are ablated.

$$d_x = \frac{v_s}{f_{rep}} \quad (1)$$

If necessary, the number of exposure layers n can be increased for a higher ablation depth z_{ab} . The resulting ablation depth z_{ab} and surface roughness Sa are measured by white light interferometry (compare chapter 4) and, based on the results, the ablation rate which describes the amount of ablated material per time is calculated according to Eq. (2).

$$\dot{V} = \frac{z_{ab} * v_s * d_y}{n} \quad (2)$$

Within this paper, the parameters listed in Table 2 are used to carry out the experiments. A unidirectional scan strategy is used in order to achieve a more homogenous energy distribution especially in the border regions of the ablated field. The number of exposure layers n is varied in order to determine the dependency of the ablation depth, the ablation rate and the surface roughness on the ablation depth and on the investigated glass materials fused silica, BK7, S-TIH6 and S-FPL53.

Table 2 Parameters used for the experiments in this paper

Beam diameter d_s [mm]	Track pitch d_y [mm]	Scan speed v_s [mm/s]	Repetition rate f_{rep} [Hz]	Pulse distance d_x [mm]	Pulse time t_{pulse} [ns]	Laser power P_L [W]	Pulse energy E_{Pulse} [mJ]	Peak power $P_{L,peak}$ [KW]
0.2	0.1	10	100	0.1	≈ 380	0.47	4.7	≈ 12

According to Table 2 it can be seen that a laser power $P_L = 0.47$ W in combination with a pulse time $t_{pulse} \approx 380$ ns is used, leading to a small pulse energy $E_{Pulse} = 4.7$ mJ and a high peak power $P_{L,peak} \approx 12$ KW. This combination leads to small thermal heating per pulse and thus small ablated volumes per pulse in short pulse time, which then should lead to homogenous material ablation regardless of the chemical composition of the processed glass material. Due to the scan speed $v_s = 10$ mm/s, test fields with the dimension of $A = 5 \times 5$ mm² are sufficient for investigating the ablation process without an influence of the acceleration or deceleration effects of the laser beam movement caused by the mirrors of the scanner system.

With these parameters, according to Eq. 3, each exposure layer needs a process time of $t_{Layer} = 25$ s.

$$t_{Layer} = \frac{A}{d_y * v_s} \quad (3)$$

With other possible parameter combinations, e.g. an increased scan speed v_s , the process time can be significantly decreased. A simultaneously increased repetition rate f_{rep} would lead to a constant track pitch d_x and so a comparable ablation result (Eq. 1). Increasing the laser power P_L would lead to higher ablation depth per pulse and thus to higher ablation rate (Eq. 2). Based on the results presented in this paper, reasonable parameter combinations for increasing the ablation rate will be examined in the future.

4. Analysis procedure

For ablation depth and roughness measurements, white light interferometry (WLI) is used. An exemplary measurement of an ablated 10x10 mm² test area is shown in Fig. 3.

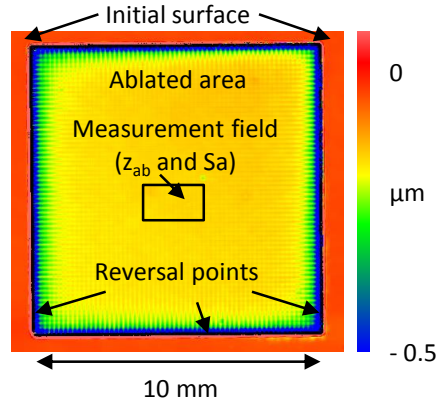


Fig. 3: White light interferometry measurement of an ablated field for measuring ablation depth and roughness [Heidrich et. al., 2014]

For identifying the ablation depth z_{ab} , a measurement field of 2×1 mm² in the middle of the sample is investigated and the height difference to the surrounding initial surface is measured. The small field size

reduces the measurement time without influencing the precision of the measurement results. More details about the analysis procedure and its reproducibility are given in [Heidrich 2014]. Despite the smaller dimensions of the ablated test fields of $5 \times 5 \text{ mm}^2$ discussed in this paper, the same procedure and same measurement field size is used for identifying the ablation depth and roughness.

5. Results

In this chapter, the results of the laser ablation by Q-switch CO_2 laser processing of different glass materials are presented and discussed. As mentioned in chapter 4, ablation depth and ablation rate as well as resulting surface roughness are analyzed.

5.1. Ablation depth and ablation rate

The ablation depth z_{ab} as well as the ablation rate in dependency of the number of exposure layers n for fused silica, BK7, S-FPL53 and S-TIH6 are shown in Fig. 4 left and right. For each layer, the parameters given in Table 2 are used.

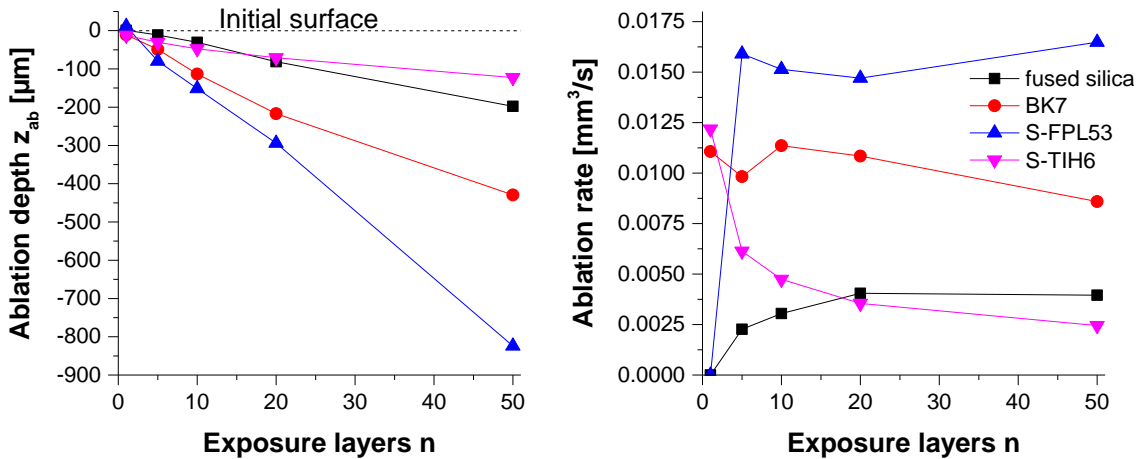


Fig. 4: Ablation depth z_{ab} (left) and ablation rate (right) in dependency of the number of exposure layers n

Starting from the initial surface, the ablation depth z_{ab} increases with increasing number of exposure layers. At $n = 50$, the highest ablation depth $z_{ab} = -824 \mu\text{m}$ is achieved for S-FPL53, the smallest $z_{ab} = -122 \mu\text{m}$ for S-TIH6. The reason for the different ablation depths might be the different amounts of energy needed for heating up and finally evaporating the different glass materials. This topic will be investigated in future experiments. Due to the small pulse energy $E_{\text{pulse}} = 4.7 \text{ mJ}$, the ablation rate only reaches values $\dot{V} \leq 0,0165 \text{ mm}^3/\text{s}$, which are given in positive values despite the ablation depth with negative values. Due to the small ablation depth regarding $n = 1$, the ablation rate for $n = 1$ cannot be precisely determined. Higher ablation rates will be achieved with higher laser power in the future.

5.2. Surface roughness S_a

The surface roughness S_a in dependence on the removed layers n for fused silica, BK7, S-FPL53 and S-TIH6 is shown in Fig. 5. For each layer, the parameters given in Table 2 are used.

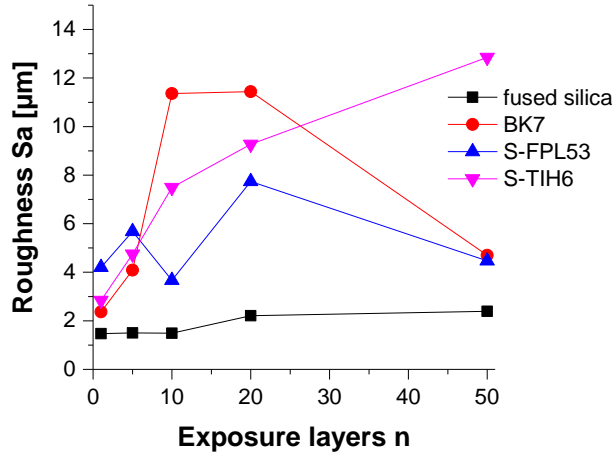


Fig. 5: Surface roughness Sa in dependency of the number of exposure layers n

Starting from a polished surface with an exemplary initial roughness of $S_a = 0.012 \mu\text{m}$ for fused silica, the roughness on each investigated glass material increases due to laser processing. At $n = 50$ and the highest investigated ablation depths, the measured roughness is between $S_a = 2.4 \mu\text{m}$ for fused silica and $S_a = 12.85 \mu\text{m}$ for S-TIH6. The reason for the roughness and the differences between the glass materials may be the different amounts of energy needed for heating up and finally evaporating the different glass materials and thus the same as for the different ablation depths. A decreased roughness may be achieved by adapting the process parameters, e.g. the pulse distance d_x and the track pitch d_y , to each glass material accordingly.

For a qualitative impression of ablated glass surfaces, exemplary WLI measurements of the initial state and ablated fields of S-TIH6 with identical scaling are shown in Fig. 6. There, in addition to Fig. 5, it can be seen that each ablated layer increases the roughness. Moreover it can be seen that the overall surface structure is not changed by increased number of exposure layers, but remains homogenous despite the different chemical elements within the glass material.

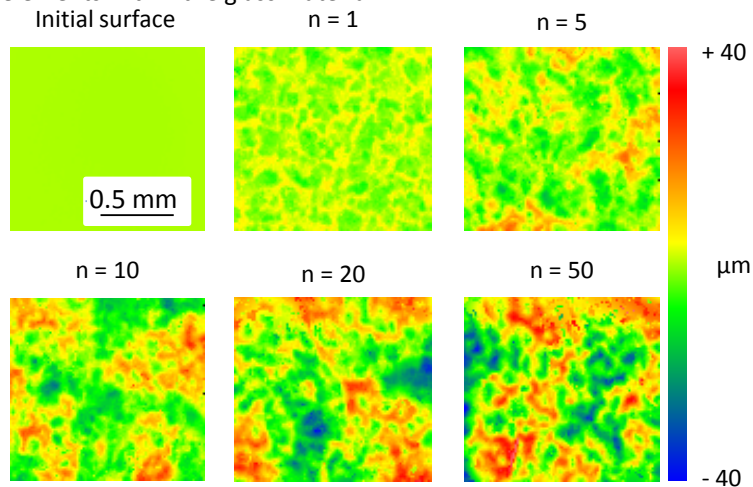


Fig. 6: White light interferometry measurement of the initial state and the ablated surfaces of S-TIH6 with identical scaling

In order to determine a possible influence of the ablation process towards the chemical composition of the processed glass materials, exemplary results of EDX-measurements of initial and ablated S-TiH6 are listed in Table 3.

Table 3: chemical analysis of the components of the initial and an ablated S-TiH6 surface (results in mass-%)

chemical element	O [%]	Na [%]	Si [%]	K [%]	Ca [%]	Ti [%]	Nb [%]	Ba [%]	Au [%]
initial surface	37.47	6.66	13.33	3.75	0.79	16.14	7.64	12.38	1.83
ablated surface (n=10)	41.18	6.80	12.08	3.52	0.76	15.06	7.32	11.95	1.33
Average	39.32	6.73	12.70	3.63	0.78	15.60	7.48	12.17	1.58
Standard deviation	2.62	0.10	0.89	0.16	0.02	0.76	0.22	0.30	0.35

Based on the results listed in Table 3, it can be seen that the initial and ablated measured surfaces exhibit a nearly identical chemical composition with only small differences. The reason for these differences is the higher roughness of the ablated material (compare Fig. 6), which leads to a different reflection angle and thereby influences the measuring result. In conclusion, the chemical composition of the initial and the ablated surface is not influenced by the ablation process.

Results of laser ablation with different numbers of exposure layers for different glass materials are shown in Fig. 7. There, the test field of BK7 with $n = 50$ and an ablation depth $z_{ab} = -430 \mu\text{m}$ on the left as well as all ablated and measured test fields of fused silica can be seen on the right. Compared to the initial polished surface of fused silica, the higher roughness of the ablated test fields, but also the high lateral resolution and edge sharpness is obvious.

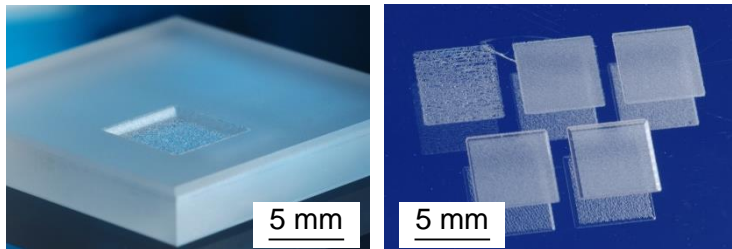


Fig. 7: Photographs of locally ablated glass materials (left) BK7 with $n = 50$ ablated layers, Processing time $t_p \approx 21$ min. (right) fused silica with ablated fields from upper left to bottom right $n = 1, 5, 10, 20, 50$.

Due to the process time per layer (Eq. 3) and the number of exposure layers $n = 50$, the overall process time for the ablated test field in Fig. 6 (left) is $t_p \approx 21$ min. In future, the process time will be decreased at least by a factor of 10 by adapting the process parameters as described in chapter 3. Moreover, compared to experiments conducted in [Nowak 2003], the ablation rate achieved within this paper is already higher by the factor ≈ 10 .

6. Conclusion and Outlook

In this paper, first results of ablating several glass materials by using a high power Q-Switch CO_2 laser source are described and discussed. Due to the wide parameter range of the laser source, especially its laser

power of $P_{Lmax,cw} = 190$ W and short pulse length of $t_{pulse} \approx 380$ ns, its main advantage compared to other laser sources are its capability of processing different glass materials without changing their chemical properties by simultaneously achieving short processing times. For the first ablation experiments, small laser power and thus small pulse energy is used. With these parameters, the different glass materials can be ablated without changing their chemical properties, which is exemplarily shown for S-TIH6. Possible applications for this approach are surface marking and ablating, e.g. for flexibly generating complex forms or for lightweight design. Moreover, when generating non-planar surfaces by locally adjusting the process parameters or the local number of exposure layers, the possible applications can be expanded to fabrication of individual freeform surfaces, e.g. for optical elements. In addition, the ablation process can be combined with a laser polishing process, which also uses CO₂ laser radiation in order to reduce the surface roughness [Richmann, 2013, Hecht, 2012].

In order to increase the process efficiency, the ablation rate will be increased in the future. Therefore, process parameters like laser power and repetition rate will be adjusted and the results will be compared to the ones presented in this paper. Because of the potential of the High Power Q-Switch CO₂ laser source, an increase of the ablation rate by the factor $> 10 \dots 100$ seems to be possible.

Acknowledgements

Parts of this work have been conducted within the RapidOptics project which is supported by the Federal Ministry of Education and Research (BMBF, 13N13294) and the project executing organization VDITZ. The above results were acquired using facilities and devices funded by the Federal State of North-Rhine Westphalia within the center for nano-photonics under grant number 290047022.

References

- Feha Lasertec GmbH, 2015. Data sheet of the Feha microstorm Q-Switch CO₂ laser source
http://www.feha-laser.de/fileadmin/user_upload/Downloads/Produktflyer_MICROSTORM.pdf
- Hecht, K., 2012. Entwicklung eines Laserstrahlpolierverfahrens für Quarzglasoberflächen, TU Ilmenau Universitätsbibliothek, ISBN 978-3863600419
- Heidrich, S., 2014. Abtragprozesse und Prozesskette zur laserbasierten Fertigung optischer Elemente aus Quarzglas, Shaker Verlag, ISBN 978-3844029260
- Heidrich, S. et al., 2014. Optics manufacturing by laser radiation, Optics and Lasers in Engineering Vol. 59 , S. 34-40, 2014
- Lee, S., 2002. Q-Switched CO₂ lasers deliver power, Industrial Laser solutions for manufacturing
- Nowak, K. M., 2003. Rapid prototyping of micro-optics for brightness restoration of diode lasers, Heriot-Watt University, Edinburgh
- Richmann, A., 2013. Polieren von Gläsern und Kunststoffen mit CO₂-Laserstrahlung, Shaker Verlag, ISBN 978-3844018882
- Staupendahl, G., 2014. A Novel Q-switched CO₂ Laser and its Applications, Laser Technik Journal
- Xie J., Pan, Q., 2011. Acousto-Optically Q-Switched CO₂ Laser, Laser Systems for Applications, 2011